Thrust Analysis of the Undulating Ribbon-Fin for Biomimetic Underwater Robots

Shuo Wang, Xiang Dong, Liu-Ji Shang

Abstract— **Biomimetic underwater robots have been paid more and more attention because of high efficiency, high maneuverability and low-noise. The undulating ribbon-fins used by rajiformes and gymnotiformes show better maneuverability than those of other fishes in turbulent water. So the undulating ribbon-fin propulsion is analyzed for biomimetic underwater robot design and optimization in the paper. The geometric model of the ribbon-fin is set up in Cartesian space. The undulating motion of the ribbon-fin is expressed in trigonometric functions. And the ribbon-fin has been divided into many small elements to compute the force acted on the small element. All the forces acted on the elements in one undulating period are summed, and the average thrust for one undulating period of the ribbon-fin is obtained. The simulation results show the influence of several important parameters on the ribbon-fin thrust. And an experimental platform is built and several experiments are carried out. And the difference between the results of simulation and experiment are discussed further.**

I. INTRODUCTION

IN the oceans which cover approximately 71% of Earth's surface, fish is one kind of amazing creatures. Comparing to traditional artificial underwater vehicles, it has advantages of greater efficiency and better maneuverability. Therefore, a lot of researches have been conducted to the propulsive mechanisms of fish to design novel underwater vehicles. The fish's swimming type can be generally divided into two categories: BCF locomotion, which generates thrust by bending fish's body into a backward-moving propulsive wave that extends to its caudal fin, and MPF locomotion, which develops alternative swimming mechanisms that involve the use of their median and pectoral fins. For achieving greater thrust and accelerations, BCF locomotion has been employed in the majority researches of biomimetic underwater vehicles. However, MPF locomotion has the advantages of greater maneuverability and better propulsive efficiency, especially at slow speeds, and attracts more and more attention. MPF propulsion mostly depends on median fin to give the thrust forces. Paired fins rarely contribute to forward propulsion and mostly supply stabilization and steering purposes. But a special propulsion system with ribbon-fins is paid more attention in recent years, which is classified into MPF. This paper will focus on the dynamic analyses of an artificial undulating ribbon-fin which is inspired by rajiform and gymnotiform (formes of MPF locomotion) fish.

A lot of researchers have done much on ribbon-fins including biomimetic mechanical design, hydrodynamic analysis, propulsion control, maneuvering and locomotion control, side-sway, etc. E.M.Standen and G.V.Lauder [1] observed and captured the fish motion in a multi-speed flow tank by means of high-speed digital cameras and gave dorsal and anal fin function during propulsion and maneuvering through statistic analyses. Dan Xia, Weishan Chen et al [2] considered the side-sway problem in rigid robotic fish and gave three restraining methods for robotic fish design to process fish body-sway, but more experiments should be carried out to verify the performance of the three methods. Michael Epstein et al [3] analyzed the structure of the ribbon fin, and designed the undulating gait of the fin. Based on the basic hydrodynamic principles, a computation model of the thrust of a robotic ribbon fin was given. Then simulations and experiments were carried out to validate the model. However the analytic solution for thrust was given. Xiang Dong et al designed a ribbon fin mechanism and built an experimental platform for the undulating long-fin research [4]. In addition, [5] concluded some basic problems of biomimetic propulsive mode. Some experiments had been carried out with a ribbon fin mechanism were concluded and some valuable results were obtained. K H Low et al developed underwater biomimetic robot with one undulating fin [6], and Yasuyuki Toda et al developed an underwater robot with side fins [7]. However, more studies have to be done to explore the mechanism of undulating ribbon-fins for designing new underwater thrusters. So the thrust generated by a ribbon-fin is analyzed in this paper. The analytic solution of the ribbon-fin's average thrust is obtained under some assumptions. And the simulations and experiments are carried out to discover how such parameters as frequency, amplitude and wave number affect the thrust. The differences between the results of simulations and experiments are discussed.

The remainder of the paper is organized as follows. Section II introduces the structure of the ribbon-fins. Section III analyzes the hydrodynamics of the undulating

This work was supported by NSFC (No. 60605026, 60725309) and 863 projects (No. 2009AA043901, 2008AA040207).

Shuo Wang, Liu-ji Shang are with State Key Laboratory of Intelligent Control and Management of Complex Systems, Institute of Automation, Chinese Academy of Sciences, Beijing 100190, China PR. (emails: shuo.wang@ia.ac.cn; fineshang@163.com)

Xiang Dong is with the Institute of Intelligent Machines, Chinese Academy of Sciences, P.O. Box 1130, Hefei City 230031, Anhui Province, China PR. (e-mail: xdong@iim.ac.cn).

ribbon-fins and gives the analytical form of thrust generated by the long-fin. Section IV discusses the simulation and experiment results. Finally the conclusion is given in section V.

II. Ribbon-fin Structure and Kinematics

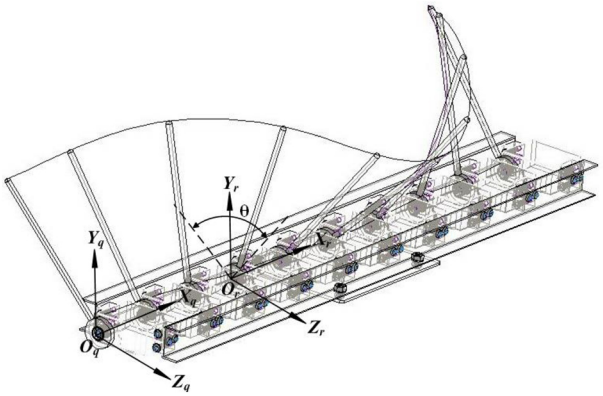

Fig.1. Ribbon-fin structure.

As shown in Fig. 1, the ribbon-fin consists of supporter, servo motor, fin ray, and membrane. Different fin rays are driven by different servo motors which are installed in the supporter. And all the fin rays are connected and covered by the membrane. The servo motors rotate according to special control strategies to drive the fin rays, and the fin rays make the membrane undulating in the water to generate thrust. For the purpose of dynamic analysis, the coordinates $O_qX_qY_qZ_q$ for the whole ribbon-fin and the coordinates $O_rX_rY_rZ_r$ for each fin ray are set up. Assumed that the fin ray motion is cyclic motion in the plane $Y_rO_rZ_r$ and expressed as below.

$$\theta(t) = \theta_m f(t) \tag{1}$$

Where θ_m is the maximal oscillating amplitude of the servo motor, $f(t)$ is the cyclic motion function. And the motion of a point on the fin ray can be described as follow with respect to the coordinates $O_rX_rY_rZ_r$.

$$\begin{cases} x_r(h,t) = 0 \\ y_r(h,t) = h\cos[\theta(t)] \\ z_r(h,t) = h\sin[\theta(t)] \end{cases} \tag{2}$$

Where h is the distance between a point on the fin ray and the origin of its fin-ray coordinates. $h \in [0, H]$. H is the length of the fin ray. t is time.

In the coordinates $O_qX_qY_qZ_q$, each fin ray has same cyclic motion expression but has its own phase related to its position on axis O_qX_q. And the motion of one point on the membrane is described as below with respect to the coordinates $O_qX_qY_qZ_q$.

$$\begin{cases} x_q(s,h,t) = s \\ y_q(s,h,t) = h\cos[\theta(s,t)] \\ z_q(s,h,t) = h\sin[\theta(s,t)] \end{cases} \tag{3}$$

Where s is the point position on axis O_qX_q, and $s \in [0, S]$. S is the length of the membrane.

The thrust of ribbon-fin is deduced on the basis of kinematic analyses in section III. And the fin ray motion is described by a cosine function.

$$\theta(s,t) = \theta_m \cos(2\pi ft - \frac{2\pi}{\lambda}s + \varphi_0) \tag{4}$$

Where f is oscillating frequency, λ is the wave length of the undulating ribbon-fin, φ_0 is the initial phase.

III. Thrust Analysis of the Undulating Ribbon-fin

The thrust of the ribbon-fin is produced by the interaction of the membrane and the fluid. The surface of the membrane is changed cyclically, so we choose one period of the ribbon-fin motion to calculate the average thrust. The whole membrane is divided into many small elements, and the forces acted on the elements in the period are calculated and summed to obtain the average thrust.

A. Basic Hydrodynamic Principle

The interaction between the small element surface and fluid is according to the following equations [8].

$$\begin{cases} \vec{f}_n = \dfrac{d\vec{F}_n}{dS} = -\dfrac{1}{2}\rho C_n \left\|\vec{V}_n\right\| \vec{V}_n \\ \vec{f}_\tau = \dfrac{d\vec{F}_\tau}{dS} = -\dfrac{1}{2}\rho C_\tau \left\|\vec{V}_\tau\right\| \vec{V}_\tau \end{cases} \tag{5}$$

Where $d\vec{F}_n$ is the normal transient force acted on the element surface, $d\vec{F}_\tau$ is the tangential transient force acted on the element surface, dS is the area of the element, ρ is the fluid density, C_n is the coefficient of the tangential drag, C_τ is the viscous drag coefficient, $\vec{V}_n$ is the transient normal velocity with respect to the fluid, $\vec{V}_\tau$ is the tangential transient velocity with respect to the fluid.

Hence the normal and tangential transient force of the ribbon-fin can be obtained by the membrane surface integral of the forces of all the elements.

$$\begin{cases} \vec{F}_n = \iint\limits_{\Omega(t)} \vec{f}_n dS \\ \vec{F}_\tau = \iint\limits_{\Omega(t)} \vec{f}_\tau dS \end{cases} \tag{6}$$

Where $\vec{F}_n$ is the normal transient force of the ribbon-fin, $\vec{F}_\tau$ is the tangential transient force, $\Omega(t)$ is the membrane surface at time t. Because the Re number of the biomimetic robot is more than 10^5, the fluid is assumed to be inviscid fluid and the viscid effect is neglected, nearly the tangential force is neglected in the paper.

B. Dynamic Analysis of the Undulating Ribbon-fin

The following dynamic analysis for the ribbon-fin is based on three assumptions: 1) the undulating motions of the fin rays make the ribbon-fin move forward straightly along axis $O_q X_q$ without any rotation; 2) the undulating motions are with respect to axis $O_q X_q$; 3) the wave number on the ribbon-fin is integer.

The position of an arbitrary point $\vec{P}$ on the membrane can be obtained according to (3). And the transient velocity of $\vec{P}$ with respect to the coordinates $O_q X_q Y_q Z_q$ can be obtained by derivation.

$$\vec{V}_{qp}(s,h,t) = \frac{\partial \vec{P}_q(s,h,t)}{\partial t} = \begin{bmatrix} 0 \\ -h\theta_t^{'} \sin\theta \\ h\theta_t^{'} \cos\theta \end{bmatrix} \tag{7}$$

Where $\theta_t^{'} = \dfrac{\partial \theta(s,t)}{\partial t} = -2\pi f \theta_m \sin(2\pi ft - \dfrac{2\pi}{\lambda} s + \varphi_0)$

If the velocity and angular velocity of the origin of the coordinates $O_q X_q Y_q Z_q$ with respect to the inertial frame are $\vec{V}_{eq} = (U_X, U_Y, U_Z)^T$, $\vec{\omega}_{eq} = (\omega_X, \omega_Y, \omega_Z)^T$ respectively, the velocity of $\vec{P}$ with respect to the inertial frame is given below.

$$\vec{V}_{ep} = \vec{V}_{eq} + \vec{\omega}_{eq} \times \vec{r}_{qp} + \vec{V}_{qp} \tag{8}$$

Where $\vec{r}_{qp}$ represents the position vector of $\vec{P}$ with respect to the coordinates $O_q X_q Y_q Z_q$.

The velocity and angular velocity of the origin of the coordinates $O_q X_q Y_q Z_q$ with respect to the inertial frame can be assumed to be $\vec{V}_{eq} = (U_X, 0, 0)^T$ and $\vec{\omega}_{eq} = (0,0,0)^T$ according the assumptions without loss of generality. Then the velocity of $\vec{P}$ with respect to the inertial frame can be expressed below.

$$\vec{V}_{ep} = \vec{V}_{eq} + \vec{V}_{qp} = \begin{bmatrix} U_X \\ -h\theta_t^{'} \sin\theta \\ h\theta_t^{'} \cos\theta \end{bmatrix} \tag{9}$$

The normal vector of $\vec{P}$ is given in (10).

$$\vec{n} = \frac{\partial \vec{P}_q(s,h,t)}{\partial s} \times \frac{\partial \vec{P}_q(s,h,t)}{\partial h} = \begin{bmatrix} -h\theta_s^{'} \\ -\sin\theta \\ \cos\theta \end{bmatrix} \tag{10}$$

Where $\theta_s^{'} = \dfrac{\partial \theta(s,t)}{\partial s} = \dfrac{2\pi}{\lambda} \theta_m \sin(2\pi ft - \dfrac{2\pi}{\lambda} s + \varphi_0)$.

The normal unit vector of $\vec{P}$ is deduced from (10).

$$\vec{n}_0 = \frac{\vec{n}}{\|\vec{n}\|} = \frac{1}{\sqrt{(h\theta_s^{'})^2 + 1}} \begin{bmatrix} -h\theta_s^{'} \\ -\sin\theta \\ \cos\theta \end{bmatrix} \tag{11}$$

And the normal transient velocity $\vec{V}_{pn}$ of $\vec{P}$ is

$$\begin{aligned} \vec{V}_{pn} &= (\vec{V}_{ep} \bullet \vec{n}_0)\vec{n}_0 \\ &= \frac{-U_X h\theta_s^{'} + h\theta_t^{'}}{(h\theta_s^{'})^2 + 1} (-h\theta_s^{'}, -\sin\theta, \cos\theta)^T \end{aligned} \tag{12}$$

Using (5), (6) and (12), the force acted on the ribbon-fin can be obtained.

$$\begin{aligned} \vec{F}_n &= -\frac{1}{2}\rho C_n \iint\limits_{\Omega} \|\vec{V}_{pn}\| \vec{V}_{pn} dS \\ &= -\frac{1}{2}\rho C_n \iint\limits_{D} \|\vec{V}_{pn}\| \vec{V}_{pn} \|\vec{n}\| ds dh \\ &= -\frac{1}{2}\rho C_n (U_X + \lambda f)^2 \iint\limits_{D} \frac{|h\theta_s^{'}| h\theta_s^{'}}{(h\theta_s^{'})^2 + 1} (-h\theta_s^{'}, -\sin\theta, \cos\theta)^T ds dh \end{aligned} \tag{13}$$

Where $D = \{(s,h) \mid 0 \le s \le S, 0 \le h \le H\}$

So the components of the force along axis X, Y, Z are expressed as follow.

$$
\begin{aligned}
F_{nX} &= \frac{1}{2}\rho C_n (U_X + \lambda f)^2 \iint_D \frac{\left|h\theta_s'\right|(h\theta_s')^2}{(h\theta_s')^2+1} dsdh \\
F_{nY} &= \frac{1}{2}\rho C_n (U_X + \lambda f)^2 \iint_D \frac{\left|h\theta_s'\right| h\theta_s' \sin\theta}{(h\theta_s')^2+1} dsdh \\
F_{nZ} &= \frac{1}{2}\rho C_n (U_X + \lambda f)^2 \iint_D \frac{\left|h\theta_s'\right| h\theta_s' \cos\theta}{(h\theta_s')^2+1} dsdh
\end{aligned} \tag{14}
$$

According to the assumptions and the characteristics of trigonometric functions, the analytical expressions can be obtained as follow.

$$
\begin{aligned}
F_{nX} &= \frac{1}{2}\rho C_n (U_X + \lambda f)^2 [2n\theta_m H^2 + \frac{n\lambda^2}{2\pi^2\theta_m}\ln^2\lambda \\
&\quad - \frac{n\lambda^2}{4\pi^2\theta_m}\ln^2(\sqrt{4\pi^2\theta_m^2 H^2 + \lambda^2} - 2\pi\theta_m H) \\
&\quad - \frac{n\lambda^2}{4\pi^2\theta_m}\ln^2(\sqrt{4\pi^2\theta_m^2 H^2 + \lambda^2} + 2\pi\theta_m H)] \\
F_{nY} &= 0 \\
F_{nZ} &= 0
\end{aligned} \tag{15}
$$

When the biomimetic robot with ribbon-fins moves forward straightly, the ribbon-fins would generate thrust along the moving orientation. And the generated thrust is related to undulating frequency, undulating amplitude, wave length, and wave number of the ribbon-fin.

IV. Simulations and Experiments

In this section, the simulations and experiments are carried out to discuss the influence of several parameters of (15). The simulation results are given according to (15). Then an experimental platform is introduced and experimental results are shown.

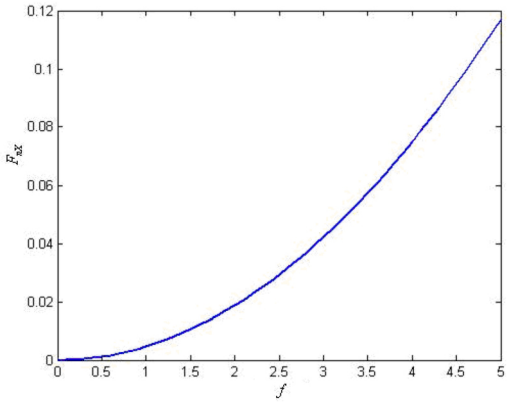

Fig.2. Thrust vs. Frequency

A. Simulation Results

The length of the membrane and the length of the fin ray are set in design. The length of the membrane is equal to the product of the wave length and the wave number of the ribbon-fin. Several parameters which are related to the mechanism and the environment are same in these simulations. The length of the fin ray is 0.12. C_n is 10. ρ is 1. The velocity U_X is zero. And the influence of such parameters as frequency, undulating amplitude and wave number are discussed respectively.

In this simulation, the maximal undulating amplitude is 0.2π and the wave number is 1. The frequency is changed from 0 Hz to 5Hz smoothly. The figure 2 shows that the thrust increases nonlinearly with the frequency increasement.

In this simulation, the frequency is 2Hz and the wave number is 1. The maximal undulating amplitude is changed from 0 to 0.5π smoothly. The figure 3 shows that the thrust increases nonlinearly with the frequency increasement.

In this simulation, the frequency is 2Hz and the maximal undulating amplitude is 0.2π. The wave numbers are set to

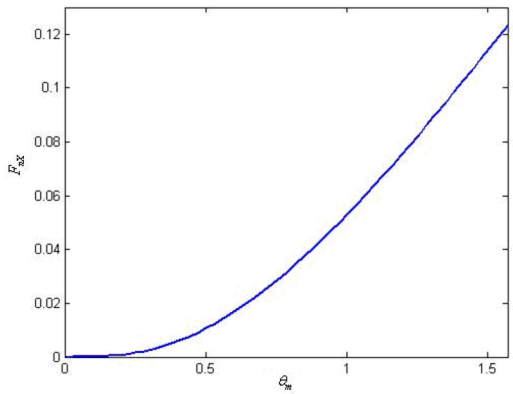

Fig.3. Thrust vs. Maximal undulating amplitude

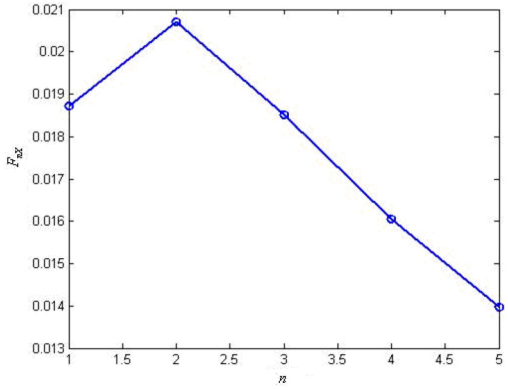

Fig.4. Thrust vs. Wave number

be 1, 2, 3, 4, and 5 respectively. The figure 4 shows that the

Fig.5. Ribbon-fin mechanism used in the experiments

thrust increases firstly and then decreases with the increasement of the wave number.

B. Experimental Results

In order to validate the analyses and simulation results, an experimental platform is built. The ribbon-fin mechanism is shown in figure 5. The servo motors are installed on two supporters. The shaft of each servo motor is connected with a rigid rod. And the membrane made of rubber covers all the rods.

The basic parameters of the ribbon-fin mechanism are given in Table I.

The experimental platform is built, as shown in figure 6. An analogue push-pull mechanical force gauge with capacity 50 N is used for thrust measurement. The resolution of the force gauge is 0.2 N and the peak holding function applies for the maximal instantaneous thrust measurement.

The experimental results are shown in figure 7. The wave number is 1 in all these experiments because of the mechanism limitation. The undulating frequency is changed from 1Hz to 3Hz, and the maximal undulating amplitude is changed from 15 degrees to 40 degrees. The thrust measurement results are maximal instantaneous thrusts, but the simulation results are average thrusts. Although the results of quantitative contrastive analysis can not be obtained by contrast of the simulation and experimental

TABLE I
PARAMETERS OF THE RIBBON-FIN MECHANISM

Membrane length	450 mm
Fin ray (rod) length	110 mm
Quantity of fin ray (rod)	10
Distance between adjacent Fin rays (rods)	50 mm
Membrane thickness	1.2 mm
Modulus of elasticity of the membrane	2.7 MPa
Servo motor	Sanwa RS995

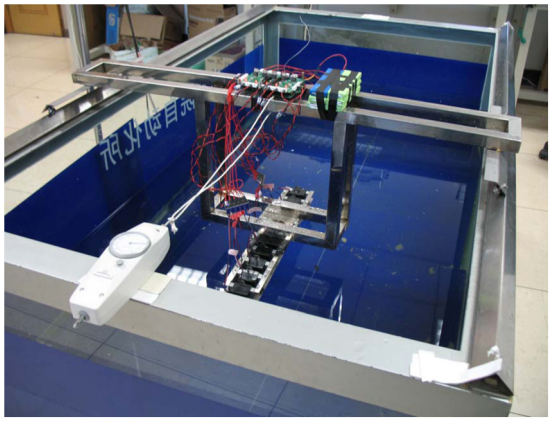

Fig.6. Experimental platform for thrust measurement of the ribbon-fin

results, the qualitative analyses can be given. The tendency of measured thrusts is similar to the tendency of the simulation results when the undulating frequency increases from 1Hz to 2.2 Hz, but different from that when the undulating frequency continues to increase from 2.2Hz to 3Hz. The similar tendency also occurs when the maximal undulating amplitude increase from 15 degrees to 40 degrees.

C. Discussions

Compared the simulation results with the experimental results, there exists differences. The reasons caused these differences may help to improve the analytic methods and design a new ribbon-fin mechanism with high efficiency and better performance.

In the thrust analyses, the effect of the membrane elasticity is not considered, which would restrict the motion of the fin rays and cause complex hydrodynamic effects. The environment disturbance does not be considered in thrust analyses either. And the parameters related to fluid characteristics for simulations are given by estimation. Generally, these parameters should be obtained through experiments.

From the view of the experiments, there are still some

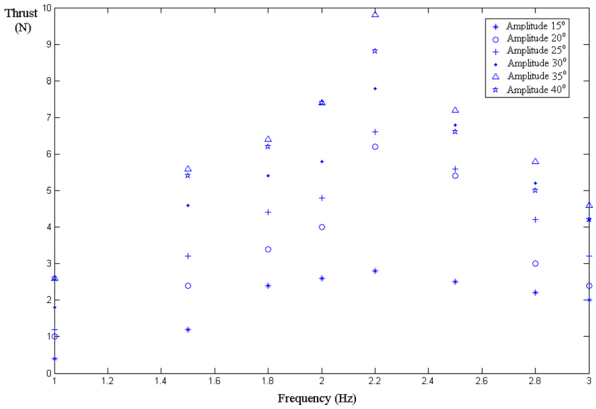

Fig.7. Experimental results

problems to be paid attention. The ribbon-fin mechanism used in the experiments need to be improved. The mechanism limitation and the response characteristics of servo motors make the ribbon-fin difficult to mimic the undulating motions perfectly, especially in the case of high frequencies and large amplitudes. The modulus of elasticity of the membrane has important influence on the thrust, but the experiments are not included in the paper. The drag acted on the ribbon-fin is difficult to measure in these experiments. And the pool used for the experiments is not big enough to reduce the influence of the wave generated by the undulating ribbon-fin.

Although there are some differences between the simulation results and the experimental results, the theoretic analyses results can help to find the reasonable range of design parameters for undulating ribbon fins to improve their performance and contribute to mechanical and controller design of the real ribbon-fins.

V. CONCLUSIONS

The thrust of an undulating ribbon-fin is discussed in the paper. The geometric model of the ribbon-fin is analyzed and the kinematics of the undulating ribbon-fin is given. The analytic solution of the average thrust is derived on the basis of geometric model and kinematics. Simulations are carried out to show the influence of frequency, amplitude and wave number on the thrust. And an experimental platform is also set up to validate the thrust analyses results. The differences between the simulation and experiment results are discussed in detail. The analyses and discussions in the paper would be helpful to optimize the ribbon-fin design for underwater biomimetic robots.

REFERENCES

[1] E. M. Standen and G.V. Lauder, Dorsal and anal fin function in bluegill sunfish *Lepomis macrochirus*: three-dimensional kinematics during propulsion and maneuvering. *The Journal of experimental Biology*, 2005, pp. 2753-2763.

[2] Dan Xia, Weishan Chen et al, "Simulation study on the body side-sway characteristic for rigid robot fish," *Robotics, Automation and Mechatronics*, Sept 2008, pp.1179-1184..

[3] Michael Epstein, J. Edward Colgate, Malcolm A. MacIver, A Biologically Inspired Robotic Ribbon Fin, 2005 IEEE/RSJ International Conference on Intelligent Robots and Systems (IROS), workshop on Morphology, Control, and Passive Dynamics. August 2, 2005, Edmonton Alberta

[4] Xiang Dong, Shuo Wang, Zhiqiang Cao, Min Tan, CPG Based Motion Control for an Underwater Thruster with Undulating Long-Fin, Proceedings of the 17th World Congress of The International Federation of Automatic Control, July 6-11, 2008, Seoul, Korea, pp.5433-5438

[5] Malcolm A. MacIver, Ebraheem Fontaine, and Joel W. Burdick, "Designing future underwater vehicles: principles and mechanisms of the weakly electric fish," *IEEE J. Oceanic Engineering*, vol. 29, no. 3, July 2004, pp.651-659.

[6] K H Low. Locomotion Consideration and Implementation of Robotic Fish with Modular Undulating Fins: Analysis and Experimental Study. Proceedings of the 2006 IEEE/RSJ International Conference on Intelligent Robots and Systems, Beijing, China, October 9 - 15, 2006, pp.2424-2429.

[7] Yasuyuki Toda, Hirofumi Ikeda and Naoto Sogihara. The Motion of a Fish-Like Under-Water Vehicle with two Undulating Side Fins. The Third International Symposium on Aero Aqua Bio-mechanisms ISABMEC 2006, July 3rd-7th, 2006, Okinawa Convention Center, Ginowan, Okinawa, Japan, paper ID: P28

[8] Kobayashi S, Kameyama T, Morikawa H. Generation of movement for multi-link prolusion mechanism in fluid. In: Proceedings of the Fourteenth International offshore and polar Engineering Conference. Toulon, France, 2004. 290-294.